2017 American Control Conference
Sheraton Seattle Hotel
May 24–26, 2017, Seattle, USA

LPV-Based Torque Control for an Extreme-Scale Morphing Wind Turbine Rotor

Dana P. Martin[1], Kathryn E. Johnson[2], Daniel S. Zalkind[3], and Lucy Y. Pao[4]

Abstract— **Recent trends in wind turbine design have demonstrated that decreased levelized cost of energy (LCOE) can be achieved by increasing rotor size and therefore the amount of energy a wind turbine can capture. However, as rotor radii increase into extreme scales, it is likely that the increased mass required to maintain the necessary structural strength for three-bladed upwind turbines will drive up costs faster than they can be outweighed by increased energy production. We are part of a team that has been working to design a two-bladed, downwind 13.2 MW wind turbine rotor that maintains structural integrity by using load alignment and active coning. Together with the increased scale and downwind configuration, the active coning provides both additional challenges and opportunities for turbine control. In this paper, we design and evaluate a linear parameter varying (LPV) generator torque control technique that compensates for the changing system dynamics as the rotor coning angle changes.**

I. INTRODUCTION

Wind energy penetration of the electricity grid has increased substantially over the past 2 decades [1], [2], and installed capacity continues to grow in both developed and developing countries around the world [1]. Emerging markets for wind and its recognition as a worldwide, economically viable, environmentally sustainable energy source allows it to be cost competitive with fossil fuel energy sources [1]. In a recent report [4], the U.S. Department of Energy outlined the necessary steps to achieve a 20% wind penetration of the U.S. electrical grid by 2030. Technological advances in material and design techniques are enabling larger rotor size and decreasing wind's Levelized Cost of Energy (LCOE).

Wind turbine control is challenging, and these challenges can be partially attributed to the energy resource itself (the wind) and its stochastic nature. In the recent past, there has been a considerable amount of advanced design of wind turbine controllers [5] - [7], increasing the efficiency and effectiveness of extracting energy from the wind. While the control advances have been made using a variety of control theories, in this paper we consider the variation of turbine dynamics a key parameter. Therefore, we have developed a Linear Parameter Varying (LPV) controller for wind turbines. LPV control is well-suited to optimize turbine performance despite model uncertainties, actuator faults, inaccurate model parameters, stochastic disturbances, measurement noise and component faults [8], [9], ensuring the turbine maintains itself within safe operating conditions given both known parameter variations and unforeseeable deviations from design criteria. References [10] - [12] use LPV control for both partial (Region 2) and full load (Region 3) wind turbine operation, utilizing the LPV framework to design a single control law that is valid across all regions of operation. The advantage in using the LPV control framework lies in its robustness and ability to be used on systems with nonlinear dynamics requiring different gains across the full envelope of operation. The ability of LPV to control nonlinear systems across wide ranges of operation, along with its robustness make it an ideal candidate for controlling novel turbine designs with uncertain dynamics.

One example of innovative turbine design is in the area of morphing rotor technology, which allows the blade geometry to morph depending on blade forces [13] - [15], thus reducing total loads at the blade root. This rearrangement of blade loads will ultimately allow for a reduction in rotor mass while simultaneously increasing energy capture [15] compared to a conventional, non-morphing rotor. A pivotal aspect of the success for load alignment technology lies in the ability of advanced control architectures to account for both the additional degree of freedom provided by the ability to actively cone the rotor and the increased blade flexibility, not accounted for in traditional torque controllers [2].

Standard wind turbine torque controllers aim to maximize power production during below-rated conditions by maximizing aerodynamic efficiency [2], [16], also known as the maximum power coefficient $C_{p_{max}}$. The maximum aerodynamic efficiency is a function of tip speed ratio λ, the rotor swept area A, and the axial induction factor a. Since active coning changes the swept area A, fixed-gain traditional torque control fails to result in a morphing rotor that operates at optimal aerodynamic efficiency. This paper, inspired by the promising results of previous LPV control strategies for wind energy, develops and analyzes a LPV strategy for this novel rotor and compares the LPV results to those obtained using a traditional baseline controller in terms of power and loads.

The paper is organized as follows: Section 2 briefly reviews the main wind turbine operating regions, the standard controller typically used in below-rated operation, and further

[1] Dana Martin is a Graduate Research Assistant at Colorado School of Mines, Division of Electrical Engineering Golden, CO 80401 USA. email: dmartin@mines.edu

[2]Kathryn Johnson is Associate Professor at Colorado School of Mines, Division of Electrical Engineering, and Joint Appointee at National Renewable Energy Laboratory Golden, CO 80401 USA. email: kjohnson@mines.edu

[3]Daniel Zalkind is a Graduate Research Assistant at University of Colorado - Boulder, Boulder, CO 80309 USA. email: daniel.zalkind@colorado.edu

[4]Lucy Pao is the Director of the Control Systems, Sensor Fusion, and Robotics Laboratory and Professor in the Department of Electrical, Computer, and Energy Engineering at University of Colorado - Boulder, Boulder, CO 80309 USA. email: pao@colorado.edu

discusses the load alignment concept and introduces a LPV system formulation. Section 3 describes the LPV controller design for below-rated operation for the morphing wind turbine. Simulation results comparing the LPV controller with a baseline controller on two turbine configurations are presented and analyzed in Section 4. Finally, Section 5 summarizes the main conclusions and briefly outlines areas for future work.

II. Background

Modern wind turbines incorporate variable speed turbine technology and have two main operating regions: below-rated (Region 2) and above-rated (Region 3). The two regions are defined based on wind speed, and the steady-state power curve corresponding to these regions which is fixed during the aerodynamic design process. Fig. 1 depicts the regions of operation for a 13.2 MW wind turbine.

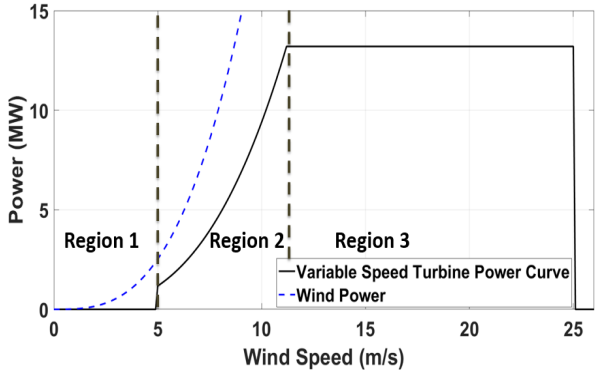

Fig. 1. Power curve for the 13.2 MW turbine. The "Wind Power" curve depicts the power available in the wind for the specified turbine (corresponding to the turbine's swept area). The wind speed at which Region 1 transitions to Region 2 is known as the "cut-in" wind speed, the wind speed corresponding to the transition between Region 2 and Region 3 is the "rated" wind speed, and the fastest wind speed before shut-down is the "cut-out" wind speed. Figure inspired by [2].

In Region 1, due to mechanical and electrical losses, it is not worthwhile to operate the turbine to generate electrical power. In Region 2, the generator torque is usually controlled so that the turbine is operated as aerodynamically efficiently as possible. In Region 3, the blade pitch is controlled to regulate the turbine at the rated power. The focus of this paper is on Region 2 operation and we review the standard generator torque controller next.

A. Standard Generator Torque Control

In below-rated operation, the generator torque is controlled to counteract the aerodynamic torque in order to maintain the tip speed ratio at its optimal value λ_*. The tip speed ratio is defined as

$$\lambda = \frac{R_a \omega}{u_d}, \tag{1}$$

where R_a is the rotor radius, ω is the rotor speed, and u_d is the free stream wind speed. The aerodynamic torque is

$$\tau_{aero} = \frac{1}{2}\rho\pi R_a^3 \frac{C_p}{\lambda} u_d^2 \tag{2}$$

where ρ is the air density, u_d is the free stream wind speed, and the power coefficient C_p is the ratio of the turbine power P_{rotor} to the available wind power P_{wind}:

$$C_p = \frac{P_{\text{rotor}}}{P_{\text{wind}}}. \tag{3}$$

A first order model for the rotor dynamics is

$$J_{rotor}\dot{\omega} = \tau_{aero} - \tau_{gen} \tag{4}$$

where τ_{gen} is the applied generator torque, τ_{aero} is the generated aerodynamic torque, and J_{rotor} is the total rotor inertia. It can be shown [3] that the following generator torque control law leads to optimal power capture in steady state:

$$\tau_{gen} = K\omega^2 \tag{5}$$

with

$$K = \frac{1}{2}\rho\pi R_a^5 \frac{C_{p_{max}}}{\lambda_*^3}. \tag{6}$$

The values for optimum tip speed ratio λ_* and maximum power coefficient $C_{p_{max}}$ are determined through aerodynamic design and modeling of the rotor. In below-rated operation, the blade pitch angles are constant and set to the optimal blade pitch for maximizing power capture.

B. Load Alignment

As rotors approach the extreme scale (>10 MW), blade mass and weight become critical design drivers [15]. The ability to continue growing rotor diameters will in turn increase energy density of wind farms, which is expected to result in an overall decrease of LCOE. A promising concept under investigation that will allow blades to be manufactured using less material and lighter structural components is the Segmented Ultra-light Morphing Rotor (SUMR) [13] [14] concept. The technology incorporates a new, active hinge at the blade root, allowing the blade to actively cone out-of-plane in order to align with the resulting force vector.

The blade loads that drive structural design consist of centrifugal, gravitational, and aero-elastic forces. The forces act in different planes, and depending on the region of operation (i.e. wind speed), different forces dominate the resulting angle (ψ) of the resultant force vector pushing the blade away from the un-coned rotor plane. During lower speed operation, the goal is to maximize swept area and focus on power capture, but as the angular velocity of the rotor increases, centrifugal and aerodynamic thrust forces increase, resulting in a misalignment of the resultant force vector with the reference plane of the rotor. During higher wind speeds the rotor plane is coned, compensating for the misalignment and lowering the induced reactionary moment at the blade

root. Fig. 2 depicts the three forces and the resultant vectors [15].

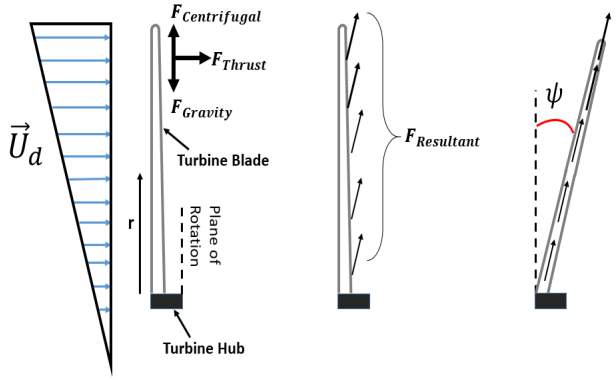

Fig. 2. The evolution of a morphing blade exposed to an axial inflow with vertical shear wind field. Initially, the blade is at rest in a vertical position and as the inflow strikes the blade, it cones downwind so that the blade becomes aligned with the resultant force due to centrifugal, thrust, and gravity forces. Fig. 2 reproduced from [15].

C. Linear Parameter Varying Systems

LPV systems are a class of systems whose describing matrices are dependent on a varying parameter $\delta \in \mathbb{R}^p$. After computing multiple LTI systems at a set of selected operating points along a desired trajectory, the LPV model is constructed using interpolation methods. The scheduling parameter δ takes values, for $t \geq 0$, that are confined to the polytope $\boldsymbol{\delta} := co\{\delta^1, ..., \delta^N\} \subset \mathbb{R}^p$. The LPV system model is given by

$$\dot{x}(t) = A(\delta)x(t) + B_d(\delta)u_d(t) + B(\delta)u(t) \quad (7)$$
$$y(t) = C(\delta)x(t) + D(\delta)u(t) \quad (8)$$

where $x \in \mathbb{R}^{n_g}$, $u_d \in \mathbb{R}^{n_d}$, $u \in \mathbb{R}^{n_u}$ and $y \in \mathbb{R}^{n_y}$. The difference between the actual power and the reference power is $e(t)$ and u_d is the wind disturbance. We design a controller such that the performance of the closed-loop LPV system minimizes the cost function

$$J(u) = \int_0^\infty (x^T Q x + u^T R u + 2x^T N u)dt \quad (9)$$

subject to (7). The matrices Q, R and N are weighting matrices used to penalize state, input, and correlation between state and input signal magnitudes, respectively. The matrices are chosen after a number of simulations used to tune the weighting matrices to achieve desired system performance.

The cost function (9) forms the basis for the controller synthesis. The LQR gain synthesis method was chosen because of its ability to satisfy multiple control requirements present in output/state feedback systems. Considering the open-loop system defined by (7)-(8), the goal is to synthesize an LPV controller taking the form:

$$\begin{bmatrix} \dot{x}_{LPV} \\ u_{LPV} \end{bmatrix} = \begin{bmatrix} A(\delta) & B(\delta) \\ C(\delta) & D(\delta) \end{bmatrix} \begin{bmatrix} x \\ \int e \end{bmatrix} \quad (10)$$

where x_{LPV} denotes the state of the controller gain and u_{LPV} is the control input command given to the plant.

III. Controller Design and Synthesis

In Section II.C, a general outline of LPV systems and the controller realization process was given. In this section, an LPV torque controller is synthesized for a 13.2 MW wind turbine with a morphing rotor. The turbine is a downwind, two bladed turbine with a rated power of 13.2 MW at a rated wind speed of 11.3 m/s. The morphing schedule is dependent on wind speed and aims to minimize flap-wise blade root bending moments across a range of Region 2 wind speeds. Equation (5) governs Region 2 torque control, but was derived for a rotor with a fixed cone angle and thus radius R_a, no longer guaranteeing optimal aerodynamic efficiency for a morphing rotor. In this section, the morphing schedule is presented along with the generalized LPV system to be used in the synthesis of a torque controller for the SUMR turbine.

A. Model Description

The LPV model is based on the steady state power curve, or the mapping of wind speed to turbine power, as shown in Fig. 3. Morphing control is performed based on a schedule of rotor cone angle vs. wind speed, as shown in Fig. 4, and can therefore be directly mapped to steady-state power.

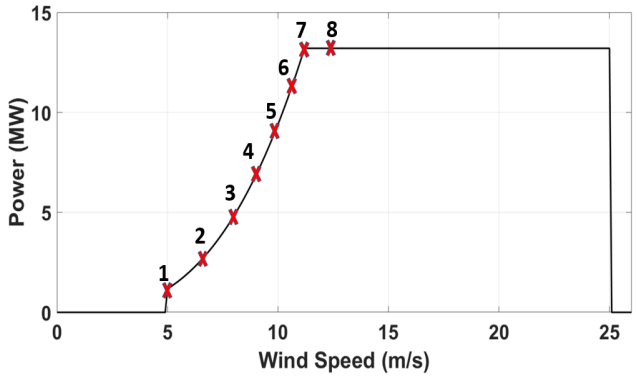

Fig. 3. Steady state operating power curve for the 13.2 MW turbine: The x's denote the operating points that are used to generate the linear time-invariant (LTI) state space matrices similar approach as in [8].

The fact that the LPV model is dependent on a scheduling variable δ that is a function of the stochastic wind speed is problematic because wind speed cannot be measured reliably at bandwidths required for controller implementation. LIDAR wind speed measurements are currently being validated by other research groups, [7], but remain uncommon in commercial wind systems and turbine power could just as easily be mapped to the high speed shaft (HSS) angular velocity, which is easily measurable. For the purposes of this paper, the power and coning angle will be derived as a function of the high speed shaft's angular velocity. Each linearization point in Fig. 3 corresponds to a steady state operating condition for the 13.2 MW turbine.

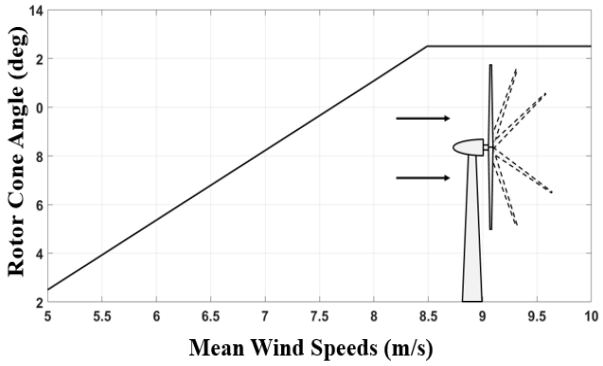

Fig. 4. Rotor coning angle ψ vs. mean wind speed used for morphing rotor simulations. The rotor begins with a downwind coning angle of $2.5°$ at the cut-in wind speed of 5 m/s, and increases linearly to a constant $12.5°$ at $0.75V_{rated}$.

The LTI state space matrices for each operating point shown in Fig. 3 are obtained using the linearization capabilities available in FAST8 [18]. A single degree of freedom, the generator shaft angular velocity, was used in the linearization process. The final LTI systems are given by (11) and (12).

$$\dot{x} = A_i x + B_i u \tag{11}$$

$$y = C_i x + D_i u \tag{12}$$

$$\text{for} \qquad i = \{1, 2, ..., 8\}$$

where $\boldsymbol{x} = \begin{bmatrix} \Delta\omega \\ \int e \end{bmatrix}$, $\boldsymbol{u} = \begin{bmatrix} u_{LPV} \\ u_d \end{bmatrix} = \begin{bmatrix} \Delta\tau_{gen} \\ \Delta V_{wind} \end{bmatrix}$, $\boldsymbol{y} = \begin{bmatrix} \Delta P \\ \Delta\omega \end{bmatrix}$.

The set of LTI state-space systems are transformed into the following affine parameter-dependent LPV system with scheduling parameter δ:

$$\begin{bmatrix} A(\delta) + jE(\delta) & B(\delta) \\ C(\delta) & D(\delta) \end{bmatrix} = \begin{bmatrix} A_0 + jE_0 & B_0 \\ C_0 & D_0 \end{bmatrix} + \delta_1 \begin{bmatrix} A_1 + jE_1 & B_1 \\ C_1 & D_1 \end{bmatrix} + ... + \delta_7 \begin{bmatrix} A_7 + jE_7 & B_7 \\ C_7 & D_7 \end{bmatrix} \tag{13}$$

IV. Implementation, Simulation, and Analysis

We use FAST8 in Matlab's Simulink® environment to simulate the response of the two-bladed downwind rotor with several controllers. Simulations are run using turbulent wind fields in below-rated (5 m/s - 12 m/s) wind speeds. The high-speed shaft's angular velocity is measured at 80Hz and a torque command is computed and applied at this sampling rate. Three configurations with two control architectures are simulated:

- LPV_{morph}: The LPV torque controller of Section III with the downwind, 2 bladed morphing rotor, where the coning angle is scheduled as show in Fig. 4. Fig. 5 depicts a block diagram of the LPV control system with its control input, controlled outputs with state feedback, and disturbances.
- BL_{morph}: The baseline generator torque controller (5) of Section II.A with the downwind 2 bladed morphing rotor, where the coning angle is scheduled as shown in Fig. 4.
- $CONR$: The standard generator torque controller (5) of Section II.A for a baseline 3 bladed upwind turbine [17] with a constant pre-cone angle of $-2.5°$, where the negative sign indicates coning upwind.

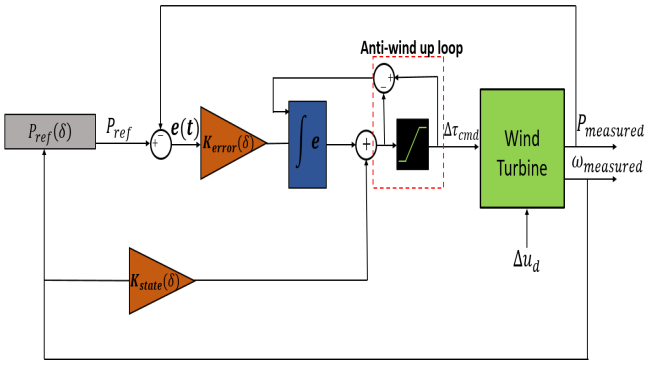

Fig. 5. LPV Block Diagram. The scheduling parameter δ is used to determine the power command $P_{ref}(\delta)$ for the output with state-feedback torque controller.

A. Power Curve Generation

The top priority for the new LPV controller is to match (or exceed) the steady-state power curve resulting from the baseline controller before any load reduction capabilities are examined. To generate power curves for each of the three turbine-controller configurations (LPV_{morph}, BL_{morph}, and $CONR$) steady state power production values were obtained for constant wind speed inputs ranging from 5 m/s to 12 m/s. Fig. 6 shows the comparison between the three test cases.

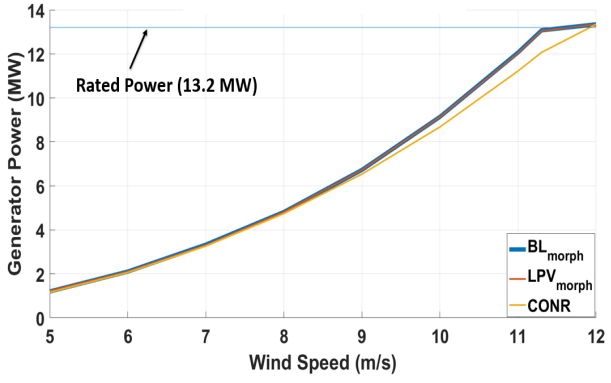

Fig. 6. Steady state power curve for the three turbine-controller configurations. The LPV_{morph} and BL_{morph} curves are indistinguishable by design.

The power curves for LPV_{morph} and BL_{morph} are identical, reaching rated power at the rated wind speed of 11.3 m/s, while $CONR$ matches power production during most of Region 2 operation, but then drops off and eventually achieves rated power at 6% above the rated wind speed.

B. Turbulent Wind Performance

The three 13.2 MW turbine-controller configurations were simulated in FAST8 using eight, 10 minute Normal Turbulence Model (NTM), class B, turbulent wind inflow fields with mean wind speeds ranging between 5-12 m/s in increments of 1 m/s. In the following sections, we show average values of generator power plotted vs. average wind speeds across the simulations in order to compare average power productions among the three test cases, Damage Equivalent Load (DEL) analysis, and time-series plots for real-time insight into the controller performance.

1) Average Power Production Comparison: SUMR technology aims to reduce blade root bending moments and rotor mass, however, without equivalent power production at equivalent scales the economic viability is lessened. In Section IV.A, the steady state power curves were matched using the BL_{morph} and LPV_{morph} configurations, but performance during turbulent wind simulations must be evaluated to fully characterize performance in realistic operating conditions. Fig. 7 shows the average power curves for the simulated turbulent wind cases.

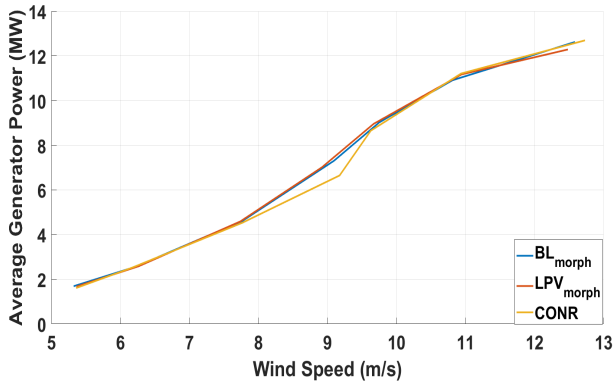

Fig. 7. Average generator power computed for each of the eight turbulent wind speed cases. Average power production is identical for the BL_{morph}, LPV_{morph} and $CONR$ except near a mean wind speed of 9 m/s where the BL_{morph} and LPV_{morph} exceed the baseline case.

The trends seen in Fig. 7 demonstrate that both the LPV_{morph} and BL_{morph} controllers match or exceed the desired power command set by the $CONR$ design power curve. With identical power production curves, the two bladed turbine is able to produce energy at a lower overall cost due to the reduction of rotor mass (i.e. less rotor mass requires less overhead capital to manufacture the turbine).

2) Lifetime Analysis: Fig. 8 shows a comparison between the DELs of various moments on the tower and Low Speed Shaft (LSS) for the BL_{morph} and LPV_{morph} controller configurations. The LPV_{morph} lowers the DEL marginally for both the side-to-side and fore-aft moments, but increases the bending and torsional moments exerted on the LSS.

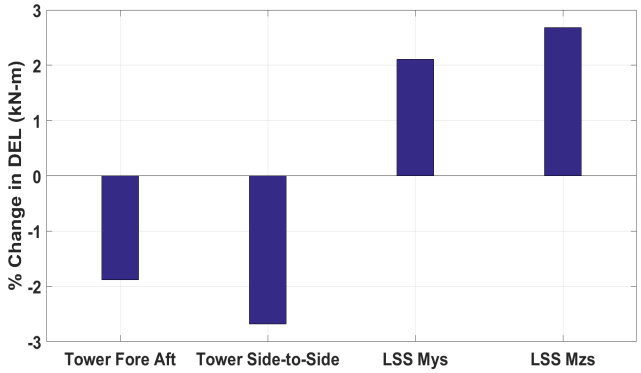

Fig. 8. Percent change of Lifetime DEL with zero mean for tower side-to-side, fore-aft, LSS bending moment, and LSS torsional moment DELs from LPV_{morph} to BL_{morph}. A negative value is the result of a lower lifetime DEL resulting from the LPV_{morph} controller.

3) Time-Series Comparison: This section presents a time-series analysis of the BL_{morph} and LPV_{morph} control architectures. Fig. 9 depicts the time-series generator power performance of the two cases for a turbulent inflow wind field with a mean wind speed of 6 m/s.

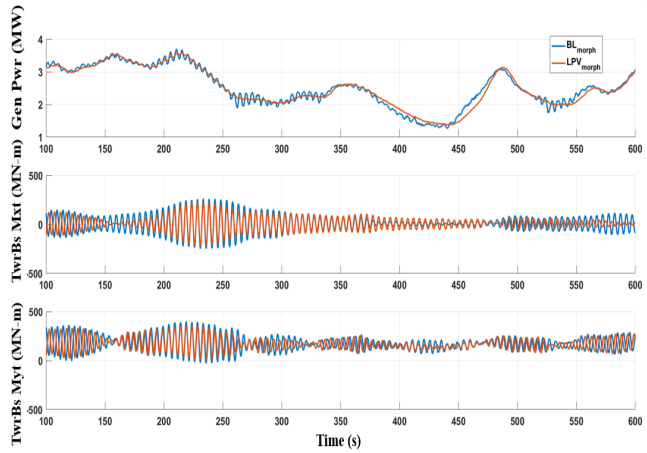

Fig. 9. Time-series plot of generator power with tower base moments for NTM wind inflow for a mean wind speed of 6 m/s.

The power production for the BL_{morph} has more oscillations and is not as smooth and the LPV_{morph}. The LPV controller has a much lower variability than the baseline case and maintains a much steadier power production. The two tower base bending moment data channels show the reduction in oscillations between the BL_{morph} and LPV_{morph} controllers. The added filtering of the LPV state-feedback control architecture reduces the oscillations of the produced power and in turn reduces the tower oscillations, further increasing the lifetime of the turbine. This result is consistent with the DEL analysis shown in Fig. 8. It should also be noted that the LPV model and controller presented in this paper did not include the tower degree of freedom or control it directly; presumably better results could be achieved if it had.

V. Conclusion

The paper describes the development of an LPV torque controller for a downwind, SUMR 13.2 MW wind turbine with a morphing rotor. The turbine and controller were then implemented in FAST8 and simulated in below-rated, turbulent and constant wind conditions. Alongside the LPV controller, two other baseline cases were simulated for comparison: a baseline torque look-up table was used for both an upwind, 3 bladed rotor with a fixed pre-cone angle of -2.5°, and an identical downwind, 2 bladed SUMR rotor. The resulting data was first analyzed using average values to observe overall trends in the controller's performance during both steady-state and dynamic simulations across a range of below-rated wind speeds. The LPV torque controller matched the power generation of the baseline, as desired. Time-series data was also analyzed to observe controller performance during a NTM wind inflow condition with a mean wind speed of 6 m/s. The power generated by the LPV torque controller had less oscillatory behavior during turbulent inflow conditions and reduced the tower oscillations in both the fore-aft and side-to-side directions. Slight tower DEL reductions also resulted, but with adverse effects on LSS moment DEL's.

The LPV controller has shown promising results in controlling a highly non linear system with increased performance in power production and tower oscillations during turbulent inflow conditions. The control architecture was constrained to Region 2 operation in this paper, and will be extended to encompass Region 3 speed regulation in future work, which will also include further load reduction and analysis.

Acknowledgment

This work has been partially supported by ARPA-E under award number DE-AR0000667 and by a Fellowship from the Hanse-Wissenschaftskolleg (HWK) in Delmenhorst, Germany. Any opinions, findings, and conclusions or recommendations expressed in this material are those of the authors and do not necessarily reflect the views of ARPA-E and HWK. The authors would also like to thank SUMR collaborators Carlos Noyes and Professor Eric Loth from University of Virginia for providing the aerodynamic morphing schedule, Gavin Ananda, Suraj Bansal and Professor Michael Selig from University of Illinois - Urbana Champaign for the SUMR aerodynamic rotor design used for the downwind, two bladed rotor configuration.

References

[1] *"World Wind Energy Report 2010"*, *in Proc. 10th World Wind Energy Conference*. Cairo, Egypt: World Wind Energy Association, Nov. 2011

[2] L. Pao and K. Johnson, *Control of wind turbines: Approaches, challenges, and recent developments*, IEEE Control Systems Magazine, Vol. 31, no. 2, April 2011, pp. 44-62

[3] K. E. Johnson and L. Y. Pao and M. J. Balas and L. J. Fingresh *Control of Variable Speed Wind Turbines: Standard and Adaptive Techniques for Maximizing Energy Capture*, IEEE Control Systems Magazine, 26(3): 70-81, June 2006.

[4] U.S. DOE Office of Energy Efficiency and Renewable Energy. 20% wind energy by 2030. http://energy.gov/sites/prod/files/2013/12/f5/41869.pdf. Accessed 09/05/16.

[5] J. Aho, P. Flemming and L. Pao, *Active Power Control of Wind Turbines for Ancillary Services: A Comparison of Pitch and Torque Control Methodologies*, American Controls Conference, 2016

[6] S. Simani, *Overview of Modelling and Advanced Control Strategies for Wind Turbine Systems*, Energies, vol. 8, 2015

[7] A. Scholbrock, P. Flemming, D. Schlipf, A. Wright, K. Johnson and N. Wang, *Lidar-Enhanced Wind Turbine Control: Past, Present, and Future*, National Renewable Energy Laboratory, NREL/CP-5000-65879, 2016

[8] S. Wang and P. Seiler, *LPV Active Power Control and Robust Analysis for Wind Turbines*, 33rd Wind Energy Symposium, AIAA SciTech, (AIAA 2015-1210)

[9] C. Sloth, T. Esbensen and J. Stoustrup, *Robust and fault-tolerant linear parameter-varying control of wind turbines*, Mechatronics, Volume 21, pgs. 645-659, 2011

[10] K. Z. Østergaard, J. Stoustrup and P. Brath, *Linear parameter varying control of wind turbines covering both partial load and full load conditions*, International Journal of Robust and Nonlinear Control, Vol. 19, pp. 92-116, 2009

[11] F. D. Adegas, J. Stoustrup, T. Knudsen, *A Framework for Structured LPV Control of Wind Turbines*, Automation and Control Section, Aalborg University

[12] V. Bobanac, M. Jelavic and N. Peric, *Linear Parameter Varying Approach to Wind Turbine Control*, 14th International Power Electronics and Motion Control Conference, 2010

[13] E. Loth, M. Selig, and P. Moriarty, *Morphing Segmented Wind Turbine Concept*, AIAA 2010-4400, 2010

[14] E. Loth, B. Icther, M. Selig, and P. Moriarty, *Downwind Pre-Aligned Rotor for a 13.2 MW Wind Turbine*, AIAA 2015-1661, 2015

[15] A. Steele, B. Ichter, C. Qin, E. Loth, M. Selig and P. Moriarty, *Aerodynamics of an Ultralight Load-Aligned Rotor for Extreme-Scale Wind Turbines*,American Institute of Aeronautics and Astronautics, 2013

[16] J. Jonkman, S. Butterfield, W. Musial and G. Scott, *Definition of a 5-MW Reference Wind Turbine for Offshore System Development*, National Renewable Energy Laboratory, NREL/TP-500-38060, 2009

[17] D. T. Griffith and P. W. Richards, *The SNL100-03 Blade: Design Studies with the Flatback Airfoils for the Sandia 100-meter Blade*, Sandia National Laboratory, SAND2014-18129, 2014

[18] J. Jonkman and M. Buhl, *FAST User's Guide*, National Renewable Energy Laboratory, Golden, Colorado, 2005

[19] G. J. Hayman and M. Buhl, Jr., *MLife User's Guide*, National Renewable Energy Laboratory, 2012

[20] M. Buhl, *MCrunch User's Guide*, National Renewable Energy Laboratory, NREL/TP-500-43139, 2008